

# Simultaneous Measurement of Velocity and Temperature in Thermal Mixing Shear Layer using LDV and Cold Wire

by

M. Hirota<sup>(1)</sup>, H. Nakayama<sup>(1)</sup>, H. Asano<sup>(1),(2)</sup>, Y. Mizuno<sup>(2)</sup>, S. Hirayama<sup>(2)</sup>

<sup>(1)</sup>Department of Mechanical Engineering

Nagoya University, 464-8603, Nagoya, Japan.

E-mail: hirota@mech.nagoya-u.ac.jp, naka@mech.nagoya-u.ac.jp

<sup>(2)</sup>CAE Center, Air-Conditioning Testing and Evaluation Department

Denso Corporation, 448-8661, Kariya, Japan.

E-mail: asano@ralg.denso.co.jp, yasuhiko\_mizuno@rnet.denso.co.jp, hirayama@rjd.denso.co.jp

## ABSTRACT

A simultaneous measurement system of the fluctuating velocity and temperature using a two-component LDV combined with a fine cold-wire thermometer has been developed, which can be potentially applied to the measurement of turbulent heat fluxes in complex turbulent airflow accompanied by reversed flow. The frequency response of the cold wire, which is affected by the thermal inertia of the wire itself and by the thermal conduction to the supporting prongs, has been compensated using the velocity data obtained by the LDV. A time lag that comes from the separation distance between the measuring points of the LDV and the cold wire has been corrected based on the hypothesis of the frozen turbulence and the cross-correlation coefficient criterion. Moreover, we propose a new measurement procedure to obtain the turbulent heat flux accurately, by which the influence of contamination of the cold wire by seeding particles for LDV (oil droplets in the present case) can be avoided.

In this paper, after describing the details of the measurement procedure, the results obtained in a near wake region behind a heated cylinder are compared with those available in an open literature to verify the reliability of the proposed simultaneous measurement technique. This comparison reveals that the proposed method can be successfully applied to the measurement of the turbulent heat flux in a wake. Next, we have applied this method to the measurement of the turbulent heat flux in thermal mixing in a planar shear layer, which simulates the thermal mixing in HVAC unit. Based on the measured results, the turbulent thermal mixing process in the planar shear layer is discussed. As future works, the present measurement technique will be applied to more complex flow geometries that simulate the HVAC unit used in automobile air-conditioning system.

## 1. INTRODUCTION

In thermal mixing process encountered in various industrial equipments, the transport of heat by turbulence is an important issue that dominates the rate of thermal diffusion and the temperature distribution in the equipments. One of the typical applications is found in an HVAC (Heating, Ventilating, Air Conditioning) unit used in an automobile air-conditioning system. The concept of the HVAC unit is illustrated in Fig.1, in which hot air heated by a heater-core and cold air cooled by an evaporator is mixed to control the air temperature blown into the compartment. The flow-rate ratio of hot and cold air, and consequently the temperature distribution in the compartment, is determined by an amount of the opening of the "air-mix door" that is installed between two heat exchangers. Thus, the hot air collides with the cold air at various angles and flow-rate ratios.

Now it is strongly desired that HVAC be designed virtually without any trial productions making the most use of CAE. Since the thermal mixing process of the hot and cold air is dominated by the turbulent heat fluxes, it is recognized that the performance of the numerical simulation (the accuracy of the simulated temperature distribution in the compartment) mostly depends on the modelling of the turbulent heat fluxes (Kitada, 2000). In general, however, the measurements of the turbulent heat fluxes in such complex flows as encountered in the HVAC unit are so difficult that reliable experimental data are quite scarce. Therefore, the modelling of the turbulent heat fluxes in the thermal mixing process is hardly adequate nowadays. Generally, the simultaneous measurement of fluctuating velocity and temperature is needed to obtain the turbulent heat flux, and it has been performed using the multi-wire probes that consist of fine cold and hot wires (Hishida & Nagano, 1978; Antonia et al., 1985; Hirota et al., 1997; Zhou et al., 2000). However, it is in principle difficult to apply this technique to the complex turbulent flow that is accompanied by the flow reversal. Hence, it is now recommended that the combination of LDV and a fine cold-wire thermometer (Heist et al., 1998; Pietri et al., 2000) be used in the measurement in the complex flow, albeit several technical problems still remain.

The main purpose of the present study is to establish a simultaneous measurement system of the fluctuating velocity and temperature using the LDV combined with the fine cold-wire thermometer, and to apply this system to the measurement of thermal mixing process inside the HVAC unit. Basically the temperature signal from the cold wire and the burst signal from the LDV are synchronized to measure the turbulent heat flux. The frequency response of the cold wire, which is affected by the thermal capacity of the wire and by the thermal conduction to the supporting prongs, has been compensated using the velocity data obtained by the LDV. A time delay that mainly comes from the separation distance between the measuring points of the LDV and the cold wire has been corrected based on the hypothesis of the frozen turbulence and the cross-correlation coefficient criterion. Moreover, a measurement procedure is proposed that enables to avoid the influence of contamination of the cold wire by seeding particles for LDV (oil droplets in the present case).

In this paper, after describing the detailed procedure of the simultaneous measurements of fluctuating velocity and temperature, the results of turbulent heat flux measured in a near wake region behind a heated cylinder are shown and they are compared with the data available in an open literature to verify the reliability of the proposed measurement technique. Then, as the first step to make clear the turbulent thermal mixing process in HVAC unit, we have applied this method to a turbulent thermal mixing in a planar shear layer. The distributions of mean velocity and temperature, turbulent shear stress and turbulent heat flux over the mixing layer are shown together with the visualized interface of two streams. The turbulent thermal mixing process in the shear layer is examined based on these measured results.

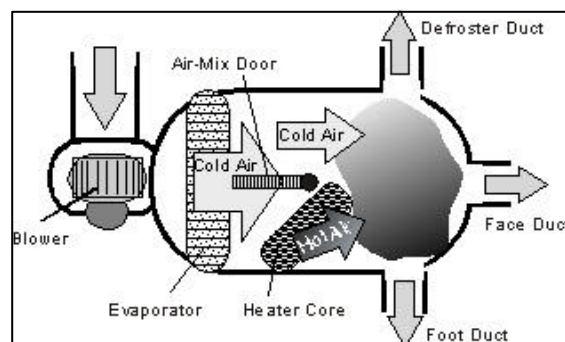


Fig. 1. Concept of HVAC unit

## 2. EXPERIMENTAL SET-UP

### 2.1 Tested flow configurations

#### Near wake behind a heated cylinder

Figure 2 shows the flow configuration and coordinate system for the near wake behind a heated cylinder. The working fluid is air. This experiment is carried out referring to that performed by Tagawa et al. (2001). An electrically heated cylinder is installed at 25mm downstream of the bell-mouth nozzle. The cylinder is made of stainless steel of 10mm in diameter ( $d$ ) and 200 mm in length, and it contains an electric heater with an output power of 400 W. The origin of the coordinate is at the center of the bell-mouth exit. The free stream velocity  $U_\infty$  is maintained at 4m/s. The Reynolds number  $Re$  based on  $d$ ,  $U_\infty$  and the kinematic viscosity of air defined with the film temperature is about 2200. The simultaneous measurement is carried out at the position of  $X_1/d = 8.5$ ; this position is equivalent to that presented in the paper of Tagawa et al. The mean velocity components in the  $X_1$ - and  $X_2$ -directions are denoted as  $U_1$  and  $U_2$ , respectively, and the fluctuating velocity components as  $u_1$  and  $u_2$ . The mean and fluctuating temperatures are denoted as  $T$  and  $t$ , respectively.

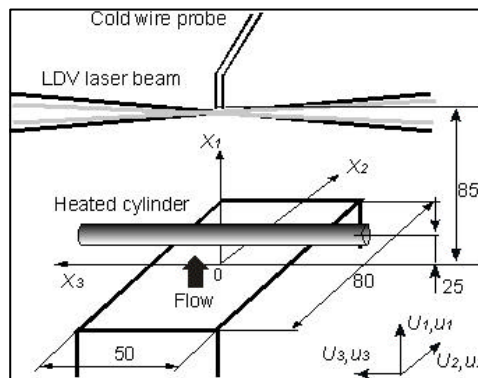


Fig.2. Experimental set-up for near wake behind a heated cylinder

#### Turbulent thermal mixing in planar shear layer

Figure 3 shows the flow configuration for the turbulent thermal mixing in a planar shear layer. After passing through settling chambers and nozzles, two streams individually form turbulent boundary layers along the splitter plate. Both the duct height and width are 200 mm ( $= 2D$ ), and the length after the trailing edge of the splitter plate (mixing section) is 700 mm. The thickness of the splitter plate, which is made of balsa, is 5 mm. The origin of the coordinate system is at the center of the trailing edge of the splitter plate;  $X_1$ ,  $X_2$ , and  $X_3$  are the streamwise, transverse, and spanwise coordinates, respectively.

The bulk velocity of the upper (cold) flow  $U_c$  is fixed at 4.3 m/s, and that of lower (hot) one  $U_h$  is 2.15 m/s. Therefore, the velocity ratio  $r (= U_h / U_c)$  is 0.5. The thickness of the boundary layer in the upper flow is about 15 mm. The temperature of the upper cold flow  $T_c$  is 303 K, and that of the lower hot flow  $T_h$  is 353 K. In this case, Richardson number based on  $U_c$  and  $2D$  is 0.0184. Therefore, the influence of the buoyancy force is negligibly small.

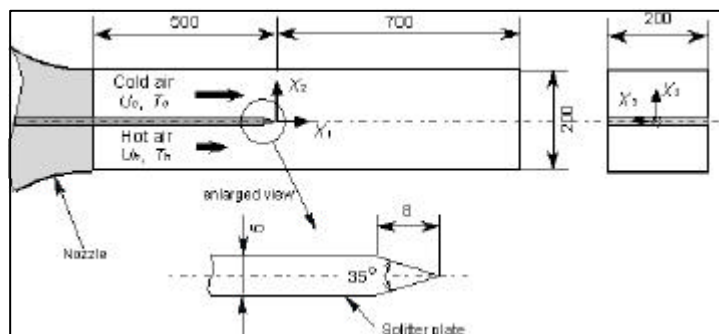


Fig. 3. Experimental set-up for thermal mixing in planar shear layer

## 2.2 Laser Doppler velocimetry

Figure 4 shows a schematic diagram of the experimental set-up for the velocity/temperature simultaneous measurement system used throughout this study. A two-component fiber optics LDV system (TSI) is used to acquire the velocity data. A 2W argon-ion laser with 488 nm and 514.5 nm lines is used as the light source. The light is transmitted from the source to the emission-reception head by 5 m long optical fibres, and the backscatter detection is used. A 350 mm focal length transmitting lens is used for the measurement. The probing volume is about 0.11 mm in diameter and 1.60 mm in length, based on  $1/e^2$  extent of light intensity. As shown in Fig.4, a reflector is used to enhance the scattered light and to form virtually the forward scatter receiver configuration.

The airflow is seeded by oil droplets (Dioctyl sebacate; density  $915\text{kg/m}^3$ ) which are generated by a Laskin nozzle (Raffel et al., 1998). The diameter of the droplets is about  $1 \sim 5 \mu\text{m}$ . The detected Doppler signal is electrically mixed with a signal derived from the driving frequency of the Bragg cell ( $1 \sim 5 \text{ MHz}$  in this experiment) and the resulting signal is processed by a signal processor (TSI IFA655). Velocity data are transferred onto a personal computer where they are processed in order to calculate the mean velocities, fluctuating velocities and their moments.

## 2.3 Cold wire thermometry

A cold-wire (CW) technique is used for the measurement of the fluctuating temperature. A tungsten fine wire with a diameter of  $5 \mu\text{m}$  is operated in a constant current (1 mA) mode. The total wire length is 5 mm; the bare center segment of 1.7 mm is the active (temperature sensing) length, and the side segments (1.65 mm long each) are plated with  $30 \mu\text{m}$  thick copper layers to be soldered with the supporting prongs as illustrated in Fig.4. The electric resistance of the tungsten wire changes with the air temperature, and it is then converted into voltage. The signal is amplified (Sokken HG-037) and continuously digitized using 16bit A/D converter (ADM-686PCI, Microscience) at a sampling rate of 10 kHz. The voltage signal is converted into temperature using the calibration curve prepared beforehand at every measurement.

In this study, the ratio of an active length of the wire sensor to the diameter  $l/d_c$  is 340. It is known that, in case of  $l/d_c < 1000$ , the heat loss through the supporting prongs of the probe as well as the thermal capacity of the fine wire affects the frequency response of the wire; the signal is contaminated by the decrease of the gain and by the phase delay (Paranthoen et al., 1982; Tsuji et al., 1992). In the present study, these effects are compensated by using the analytically based transfer function derived by Tsuji et al. (1992), which accounts for both the thermal inertia of the active sensor element and the thermal conduction toward the supporting prongs. This compensation needs the flow velocity at which the temperature is measured. As described later, the primary flow velocity measured by LDV is adopted as a characteristic velocity for this compensation.

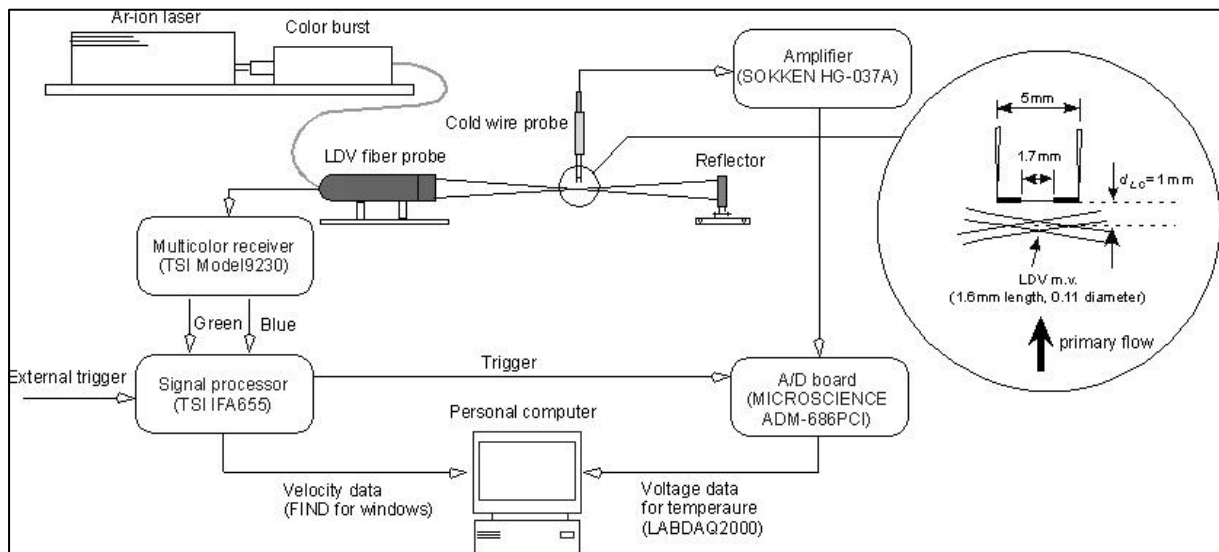


Fig. 4. Schematic diagram of the simultaneous measurement system for velocity and temperature

### 3 MEASUREMENT PROCEDURES

#### 3.1 Synchronization

Both the velocity data from LDV and the temperature signal from the cold wire sensor (CW) are acquired simultaneously and post-processed by a personal computer. Figure 5 shows a timing diagram for the simultaneous measurements of fluctuating velocity and temperature.

In this system, the signal processor of the LDV is first started by an external trigger, then the A/D converter for CW thermometer is started when the first burst signal is detected by LDV. As shown in Fig. 5 (b), the signal processor of the LDV system reads out TTL-level output when the amplitude of the Doppler signal exceeds the threshold, and the first output is used as an external trigger for the A/D converter to adjust the starting lines ( $t = 0$ ) of the velocity and temperature samplings. The time intervals between the velocity signals measured by LDV are quite random as observed in Fig. 5 (a), and the signal processor records the time at which each velocity signal is acquired (time-stamp function, Fig. 5 (b)). After obtaining 3000 realizations, the velocity data and their acquisition timings are transferred to the computer. The output from the CW amplifier is digitized with a high frequency of 10 kHz and is stored in the computer as a nearly continuous signal until LDV finishes sampling 3000 velocity data (Fig. 5 (c)). This signal from CW is then converted to the instantaneous temperature with a compensation of frequency response based on the method of Tsuji et al. as described in Sec. 2.3. The primary flow velocity is used as a characteristic velocity for this compensation.

Then, the correlation between the fluctuating velocity and temperature is calculated; the instantaneous temperature at which each velocity signal is acquired is found using the time-stamp function of the LDV signal processor. As shown in Fig. 4, however, the sensing part of the CW probe is positioned 1 mm downstream from the measuring volume of LDV to avoid any fluid dynamical and optical disturbances. This distance between the CW and LDV measuring volume brings about a phase shift between the temperature and velocity signals, and causes an error in the measured values of the turbulent heat flux. In order to keep simultaneity of the data acquisitions and avoid this error, the time lag between the velocity and temperature signals must be compensated. To estimate this time lag, we introduce a cross-correlation coefficient criterion. The cross-correlation coefficient  $R_{u_i t}$  between the fluctuating velocity  $u_i$  and fluctuating temperature  $t$  is defined as follows,

$$R_{u_i t} = \frac{\overline{u_i t}}{u_i' t'} \quad (1)$$

where the influence of the frequency response of CW on  $t$  is assumed to be already compensated.  $u_i' (= (\overline{u_i^2})^{0.5})$  and  $t' (= (\overline{t^2})^{0.5})$  represent root-mean-square (rms) values of  $u_i$  and  $t$ , respectively. This coefficient should be maximized when the synchronization between  $u_i$  and  $t$  is satisfied. As shown in Fig. 5 (d), the starting time of the compensated temperature is displaced intentionally by  $t_d$  (time delay), and the change of  $R_{u_i t}$  against  $t_d$  is calculated. Figure 6 shows an example of the dependence of  $R_{u_i t}$  on  $t_d$ , which was obtained in the planar thermal mixing layer. The value of  $R_{u_i t}$  attains the maximum at  $t_d = 1.8$  msec., and this time lag agreed well with that calculated based on Taylor's hypothesis of the frozen turbulence. This means that this criterion of the synchronization is a reasonable approach; thus this synchronizing technique has been used in the measurement of turbulent heat fluxes throughout this study.

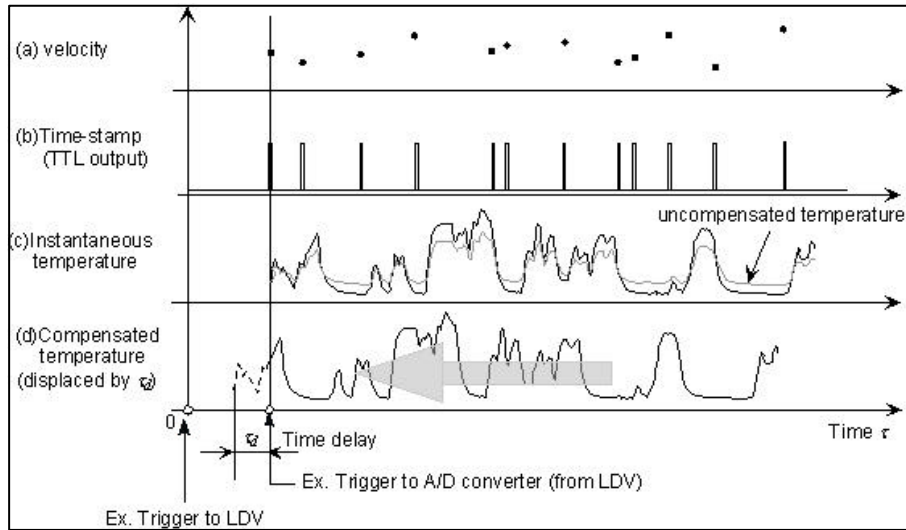


Fig. 5. Timing diagram for simultaneous measurements of velocity and temperature.

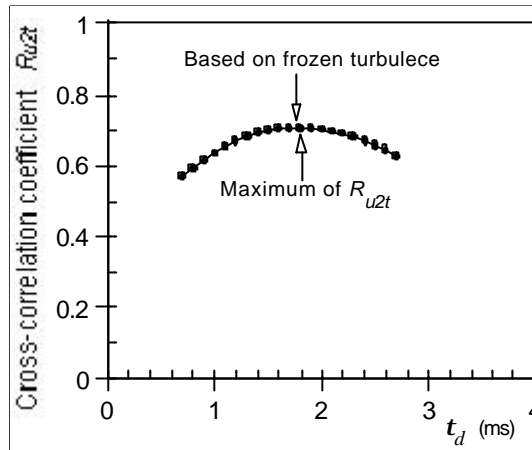


Fig. 6. Dependence of cross-correlation coefficient on time delay

### 3.2 Influence of contamination of CW by seeding particles

It is known that the cold wire thermometer is significantly affected by seeding particles (Pietri, 2000). If the wire surface is contaminated with seeding particles, the frequency response of CW is gradually deteriorated because of the increase of the thermal inertia and the decrease of the thermal conductance. Figures 7 (a) and 7 (b) show examples of the temporal variations of the power spectra and rms values of the fluctuating temperature that were measured near wake behind a heated cylinder. In this case, the airflow was seeded by oil droplets. A clean CW was exposed to the contaminated air and the temperature measurement was continued for 10 minutes in it, then the wire was cleaned up and the temperature was measured again in the contaminated air. The cold wire was cleaned with acetone in an ultrasonic bath.

It is clear from Fig.7 that the frequency response of CW thermometer to the temperature fluctuation is gradually deteriorated as the measuring (exposure) time goes by, and this is remarkable in the frequency range higher than 70 Hz. The rms value of  $t$  also decreases gradually, and the value obtained after 10-minute exposure is about 20% lower than the initial (clean CW) value. It should be noted that, since the frequency response of CW depends on the tracer density, the seeding particles should be supplied to the airflow as dilute as possible to mitigate their deposition over the wire surface.

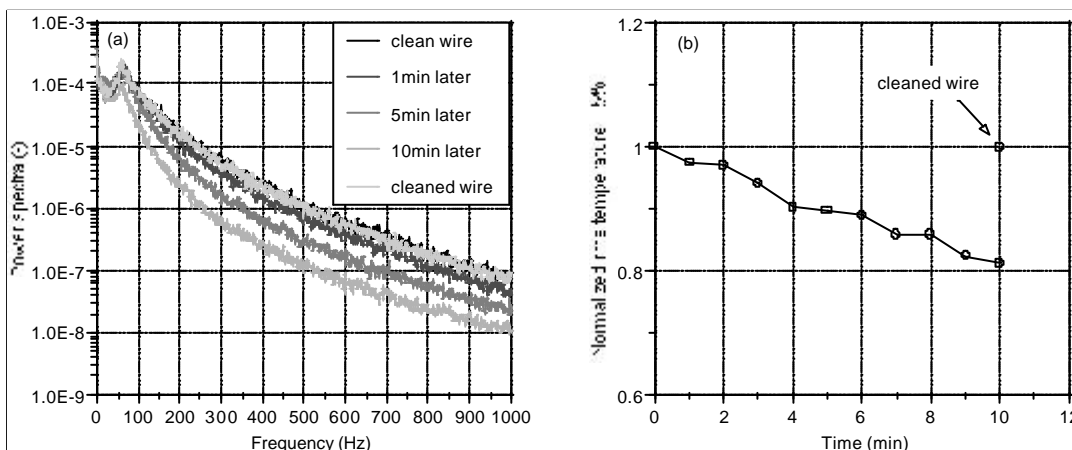


Fig. 7. (a) Temporal variation of power spectra of fluctuating temperature after the exposure to the seeded airflow  
(b) Temporal variation of rms values of fluctuating temperature

### 3.3 Measurement procedure of turbulent heat flux

The simultaneous measurements of the fluctuating velocity and temperature by the combination of LDV and CW allow the turbulent heat flux to be determined. As described above, however, the measured values of the turbulent heat flux may include serious error unless the influence of the contamination of CW by seeding particles is removed, because the measured value of  $t'$  gradually decreases as a result of seeding deposition over the wire. In order to avoid this error, we propose the following procedure to measure the turbulent heat fluxes.

As described in Sec. 3.2, the influence of the adhered particles on the CW output becomes serious in relatively high frequency range. Considering that the correlation between the fluctuating velocity and fluctuating temperature can be stronger in large eddies with relatively low frequency rather than in small eddies with high frequency, it is expected that the correlation coefficient  $R_{u't'}$  defined in Eq. (1) is less sensitive to the deterioration of the frequency response of CW than  $t'$ . In order to examine the validity of this consideration, we have measured  $R_{u'2t'}$  behind the heated cylinder for ten minutes (the same condition as that for Fig. 7) and show its temporal change in Fig. 8. It is confirmed that the values of  $R_{u'2t'}$  are almost constant for the duration of the measurement, suggesting that the influence of the contamination of CW on  $R_{u'2t'}$  is negligibly small.

On the basis of this result, the following procedure is proposed to measure the turbulent heat flux in steady turbulent flow. Here, for instance, the sequence of measuring  $\overline{u_2 t'}$  in the planar thermal mixing layer is explained.

[1] First, the mean (primary flow) velocity  $U_1$  and rms value of the fluctuating velocity  $u_2$  (usually the transverse component) are measured by LDV. Only LDV is used in this measurement (without connection with CW thermometer).

[2] Next, the mean and fluctuating temperature is measured by CW thermometer under seeding-free condition, i.e., in clean airflow. This temperature measurement is carried out with CW only and separately from LDV signal sampling. The frequency response of CW outputs is compensated using  $U_1$  obtained in the above-mentioned measurement, then the rms of the fluctuating temperature  $t'$  is calculated.

[3] The cross-correlation coefficient  $R_{u'2t'}$  is obtained by conducting the simultaneous measurements of  $u_2$  and  $t'$  with LDV and CW, which are synchronized by the method explained in Sec. 3.1. The compensation of the frequency response of CW is also performed using  $U_1$  obtained in [1], and the value of  $R_{u'2t'}$  is obtained considering the time lag ( $t_d$ ) between the sampling timings of  $u_2$  and  $t'$  as described in Sec. 3.1. In order to suppress the contamination of CW, the concentration of seeding particles for LDV should be kept as low as possible.

[4] Finally the turbulent heat flux  $\overline{u_2 t'}$  is given as the product of  $R_{u'2t'}$  (obtained in [3]),  $u_2'$  (in [1] or [3]), and  $t'$  (in [2]) that are measured separately as described above.

$$\overline{u_2 t'} = R_{u'2t'} \cdot u_2' \cdot t' = \frac{\overline{u_2 t'}}{u_{2s}' \cdot t_s'} \cdot u_2' \cdot t' \quad (2)$$

It should be noted that, since this procedure needs three separate measurements under the same experimental conditions to obtain the turbulent heat flux, it is applicable to steady turbulent flow only.

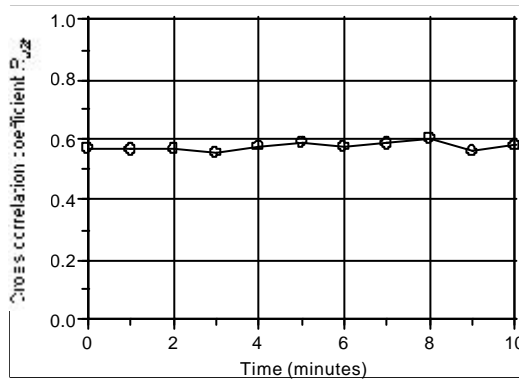


Fig. 8. Temporal variation of the cross-correlation coefficient  $R_{u'2t'}$

## 4. RESULTS AND DISCUSSION

In this chapter, the results of two experiments are described. The first one is the measurement of near wake behind a heated cylinder (Fig. 2); this experiment was performed to examine the validity of the proposed procedure for the measurement of turbulent heat flux. The second one was carried out for turbulent thermal mixing in a planar shear layer that simulates the HVAC unit used for automobile air-conditioning system.

### 4.1 Validation of the proposed technique

In order to validate the measurement technique proposed above, we compared the results obtained in a near wake flow behind a heated cylinder with the data obtained in an open literature. Basically, the experiment was conducted under the same condition as that reported by Tagawa et al. (2001), who had measured the velocity and temperature fields behind the heated cylinder by the combination of three-wire temperature probe (two thermocouples and one cold wire) and LDV. Figures 9 (a), (b) and (c) show the normalized mean streamwise (primary flow) velocity  $U_1^*/\Delta U_1 (= U_1 - U_1(\text{min})/\Delta U_1)$ , rms of the streamwise fluctuating velocity  $u_1'/\Delta U_1$ , and rms of the transverse fluctuating velocity  $u_2'/\Delta U_1$ , respectively; all the values were measured at  $8.5d$  downstream of the heated cylinder under the Reynolds number of 2200.  $\Delta U_1$  denotes the difference between the maximum and minimum streamwise velocities. It appears that the distributions of  $U_1^*/\Delta U_1$ ,  $u_1'/\Delta U_1$ , and  $u_2'/\Delta U_1$  are in good agreement with the results reported by Tagawa, albeit slight difference is observed in the level of  $u_2'/\Delta U_1$ . An off-axis peaks can be observed at  $X_2/d = \pm 1$  in both  $u_1'$  and  $u_2'$ . These features agree with those reported by Zhou et al. (1994) as well.

The distributions of the mean temperature  $T^*/\Delta T$  and the fluctuating temperature  $t'/\Delta T$  are presented in Figs. 9 (d) and (e), where  $\Delta T$  denotes the mean temperature deficit ( $= 17^\circ\text{C}$  in the present experiment). Although the present results agree qualitatively with those of Tagawa et al., quantitative difference is observed in the distribution of  $t'/\Delta T$ ; the maximum value obtained in the present measurement is about 0.38 while that reported by Tagawa is 0.51. Such a discrepancy of  $t'/\Delta T$  may come from the difference of the thermal boundary conditions such as the cylinder temperature, wall heat flux, and the ambient air temperature.

Figures 9(f) and 9(g) show the normalized turbulent shear stress  $\overline{u_1 u_2}'/U_1^2$  and the turbulent heat flux  $\overline{u_2 t}'/U_1 T$ . The principal features of  $\overline{u_1 u_2}'/U_1^2$  and  $\overline{u_2 t}'/U_1 T$  are in agreement with the published results, although the peak values of  $\overline{u_2 t}'/U_1 T$  in the present measurement are smaller than those of Tagawa et al. This disagreement reflects the quantitative difference of  $t'/\Delta T$  described above. These profiles of the turbulent shear stress and turbulent heat flux show reasonable anti-symmetry with respect to the geometrically symmetric plane ( $X_2/D = 0$ ).

From these experimental data, the turbulent Prandtl number defined by the following equation has been evaluated and the distribution is shown Fig. 9 (h).

$$Pr_t = \frac{\mathbf{n}_t}{\mathbf{a}_t} = \frac{-\overline{u_1 u_2}'/(\partial U_1/\partial X_2)}{-\overline{u_2 t}'/(\partial T/\partial X_2)} \quad (3)$$

Here,  $\mathbf{n}_t$  and  $\mathbf{a}_t$  represent the eddy viscosity and the eddy thermal diffusivity, respectively. The velocity and temperature gradients were calculated based on the least-square fitting curves to  $U_1^*$  and  $T^*$ . The present  $Pr_t$  is mostly consistent with the results of Tagawa (2001) in the wake center region, albeit some scatterings are observed in both data. In general, the value of  $Pr_t$  changes depending on the flow configuration, and the values of 0.5 ~ 0.7 are recommended in the wake region (Kays, 1994). The present result is also consistent with these recommended values and, considering the difficulty in evaluating  $Pr_t$ , it is ascertained that the measuring procedure proposed in this study is sufficiently reliable for the measurement of turbulent heat flux.

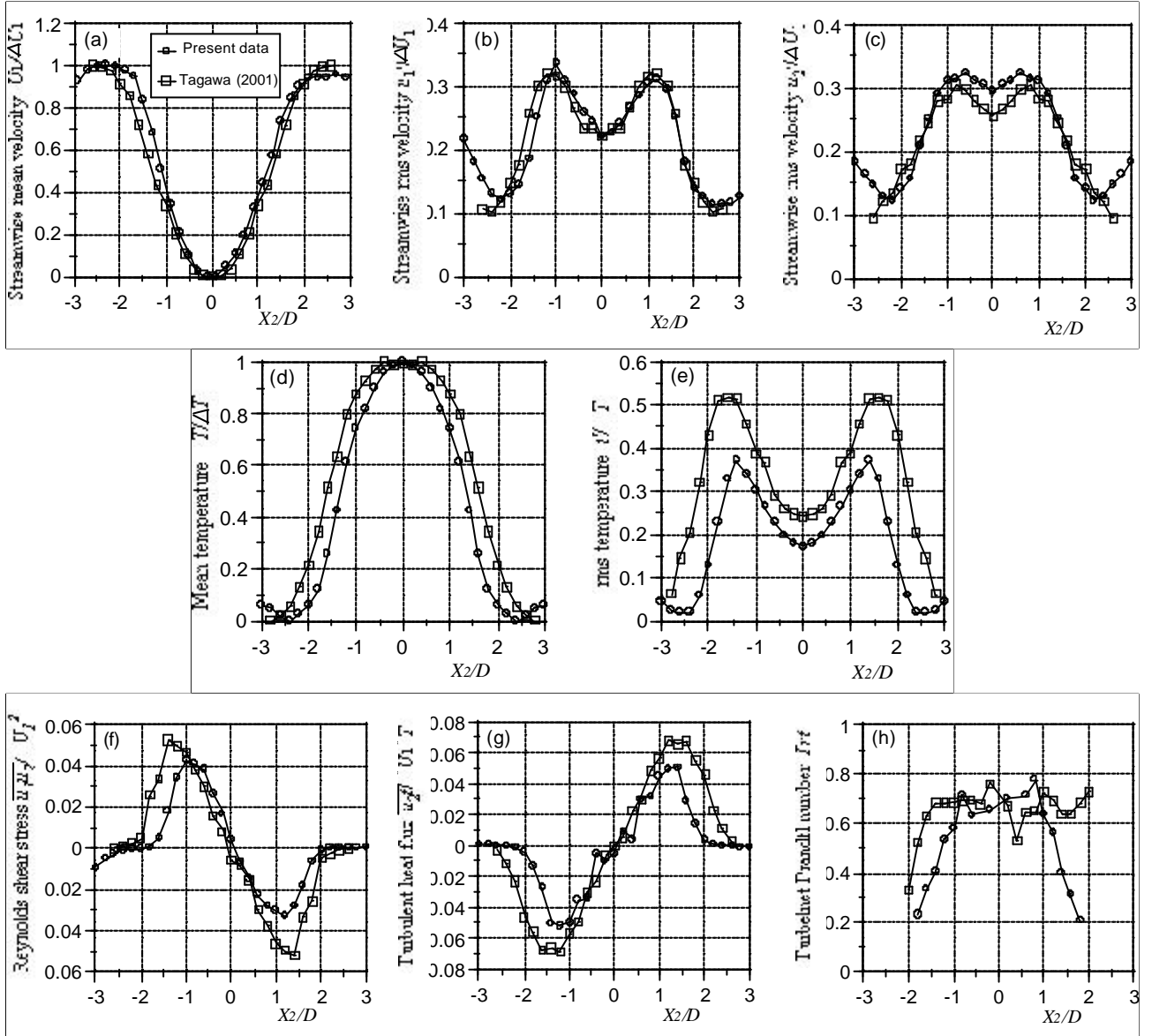


Fig. 9. Comparison with the results of Tagawa et al. (2001) (a) mean streamwise velocity  $U_1^*/DU_1$ , (b) rms of streamwise fluctuating velocity  $u_1'/DU_1$ , (c) rms of the spanwise fluctuating velocity  $u_2'/DU_1$ , (d) mean temperature  $T^*/DT$ , (e) rms of fluctuating temperature  $t'/DT$ , (f) turbulent shear stress  $\overline{u_1 u_2}/U_1^2$ , (g) turbulent heat flux  $\overline{u_2 t}/U_1 T$ , (h) turbulent Prandtl number  $Pr_t$

#### 4.2 Turbulent statistics of the planar mixing layer

Next, some results on the turbulent thermal mixing in the HVAC unit obtained with the above-mentioned measurement technique are presented. As the first step to make clear the thermal mixing process in HVAC, a planar mixing layer has been investigated with the experimental set-up shown in Fig. 3.

The distributions of the normalized streamwise mean velocity  $U_1/U_c$  measured at four streamwise locations of  $X_1/D = 0.35, 0.5, 1.0$  and  $2.0$  are shown in Fig.10. The velocity defect is observed around the plane of  $X_2/D = 0$  at  $X_1/D = 0.35$  and  $0.5$  but it recovers quite rapidly after  $X_1/D = 1.0$ , suggesting that the momentum exchange between the high and low speed flows is enhanced in a relatively downstream region of the shear layer. Although it is known that the velocity distribution in the developed planar shear layer shows self-similarity with a linearly growing thickness (Ho, 1984), it is not observed in the present flow to the end of the measuring section. Figure 11 shows the distributions of the mean temperature  $T^*/DT = (T-T_c)/DT$ , where  $DT$  denotes the initial temperature difference between the hot (lower) and cold (upper) flows. The thermal mixing layer develops as the flow proceeds downstream, and this development seems to be accelerated in the region after  $X_1/D = 1.0$ .

Figures 12 and 13 show the distributions of the turbulent shear stress  $\overline{u_1 u_2} / U_c^2$  and turbulent heat flux  $\overline{u_1 T} / U_c \Delta T$ , which dominate transports of momentum or heat from high to low speed (or temperature) flows. The absolute values of  $\overline{u_1 u_2} / U_c^2$  become larger as the flow proceeds downstream. This means that the turbulent momentum transport is more active in a region relatively far from the flow merging point, and this is consistent with the distributions of  $U_1 / U_c$  described above. The turbulent heat flux  $\overline{u_1 T} / U_c \Delta T$  attains the local maximums around the interface between the high and low temperature flows ( $X_2 / D = 0$ ), and it is relatively small at  $X_1 / D = 0.35$  and  $0.5$  then increases rapidly after  $X_1 / D = 1.0$ . Similar to the case of the momentum transport, such a behavior of the turbulent heat flux means that turbulent thermal mixing is promoted in a relatively downstream region and it well corresponds to the mean temperature distribution shown in Fig. 11.

To clarify such developments of the turbulent shear stress and heat flux, the mixing interface has been visualized by supplying smoke to the low speed flow. As observed in Fig. 14, the interface is smooth as far as  $X_1 / D = 0.5$  and large vortical structures caused by Kelvin-Helmholtz type instability emerge in a downstream region. It is thought that the increases of  $\overline{u_1 u_2} / U_c^2$  and  $\overline{u_1 T} / U_c \Delta T$  closely reflect this evolution of vortical structures at the interface, and this assures that the present measurement technique is applicable in the flow accompanied by such large-scale fluctuations.

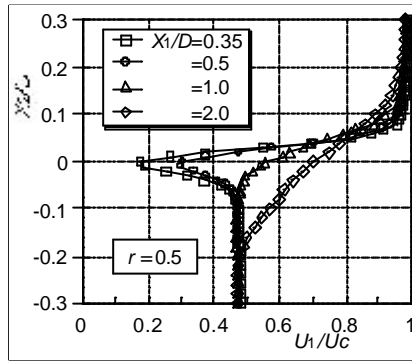


Fig. 10. Mean streamwise velocity  $U_1 / U_c$

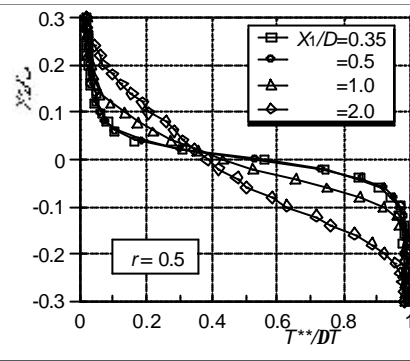


Fig. 11. Mean temperature  $T^{**} / \Delta T$

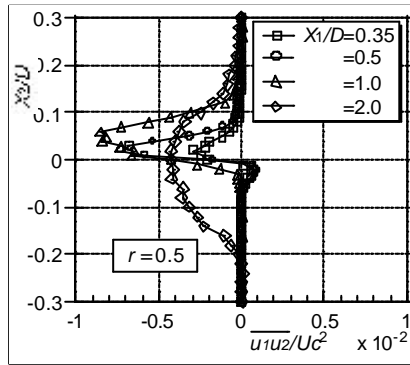


Fig. 12. Turbulent shear stress  $\overline{u_1 u_2} / U_c^2$

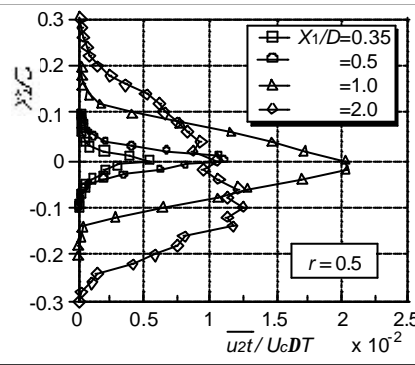


Fig. 13. Turbulent heat flux  $\overline{u_1 T} / U_c \Delta T$

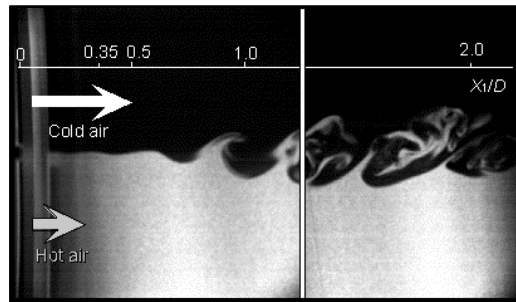


Fig. 14. Visualization of the mixing interface

## 5. CONCLUDING REMARKS

In the present study, we developed the simultaneous measurement system of the fluctuating velocity and temperature using a two-component LDV combined with a fine cold-wire thermometer, which can be potentially applied to the measurement of turbulent heat fluxes in complex turbulent airflows inside the HVAC unit. In particular, we proposed a measurement procedure to avoid the errors caused by the deposition of seeding particles (oil droplets) for LDV on the cold wire.

At first, to validate the measurement procedure developed, we measured the turbulent heat fluxes in a turbulent near wake behind a heated cylinder, and the results were compared with ones available in an open literature. It was confirmed that the measured distributions of the turbulent heat flux and turbulent Prandtl number were consistent with those reported in the previous study, and this demonstrates that the measurement procedure proposed in this study is sufficiently reliable for the measurement of turbulent heat flux in a complex flow.

Next, as the first step to investigate the thermal mixing process in HVAC unit, the measurement procedure developed in this study was applied to turbulent thermal mixing in a simple planar shear flow. The distributions of mean velocity, temperature, turbulent shear stress and turbulent heat flux over the thermal mixing layer have been measured, together with the visualization of the interface between the high and low speed flows. It was found that the vortical structure at the mixing interface has a remarkable effect on the turbulent transports of momentum and heat after the confluence of two streams. As future works, the present measurement technique will be applied to the turbulent thermal mixing in more complex flow geometries that simulate the HVAC unit used in automobile air-conditioning system.

## REFERENCES

- Antonia, R.A., Zhou, Y., and Matsumura, M. (1993). "Spectral characteristics of momentum and heat transfer in the turbulent wake of a circular cylinder", *Experimental Thermal Fluid Science*, 6, pp.371-375.
- Heist, D.K., and Castro, I.P. (1998), "Combined laser-doppler and cold wire anemometry for turbulent heat flux measurement", 24, pp.375-381.
- Hishida, M., Nagano, Y. (1978), "Simultaneous measurements of velocity and temperature in nonisothermal flows", *Journal of Heat Transfer*, 100, pp.340-345.
- Hirota, M., Fujita, H, Yokosawa, H. Nakai, H., and Itoh, H. (1997) "Turbulent heat transfer in a square duct", *International Journal of Heat and Fluid Flow*, 18, pp.170-180.
- Ho, C.-M. and Huerre, P. (1984) "Perturbed free shear layers", *Annual Review of Fluid Mechanics*, 16, pp.365-422
- Kays, W.M. (1994). "Turbulent Prandtl number – where are we?", *Transactions of ASME: Journal of heat transfer*, 116, pp.284-295.
- Kitada, M., Asano, H., Kanbara, M., and Akaike, S. (2000). "Development of Automotive Air-Conditioning System Basic Performance Simulator: CFD Technique Development", *JSAE Review*, 21, pp.91-96.
- Tagawa, M., Nagaya, S., and Ohta, Y. (2001). "Simultaneous measurement of velocity and temperature in high-temperature turbulent flows: a combination of LDV and three-wire temperature probe", *Experiments in Fluids*, 30, pp.143-152.
- Tsuji, T., Nagano, Y., and Tagawa, M. (1992). "Frequency Response and Instantaneous Temperature Profile of Cold-Wire Sensors for Fluid Temperature Fluctuation Measurements", *Experiments in Fluids*, 13, pp.171-178.
- Paranthoen, P., Petit, C., Lecordier, J.C. (1982). "The effect of the thermal prong wire interaction on the response of a cold wire in gaseous flows (air, argon, helium)", *Journal of Fluid Mechanics*, 124, pp.457-473.
- Pietri, L., Amielh, M., and Anselmet, F. (2000). "Simultaneous measurements of temperature and velocity fluctuation in a slightly heated Jet combining a cold wire and laser doppler anemometry", *International Journal of Heat and Fluid Flow*, 21, pp.22-36.
- Raffel, M., Willert, C., and Kompenhans, J. (1998), "Particle Image Velocimetry", Springer Verlag, pp.13-21.
- Zhou, Y., So, R.M.C., Liu, M.H., Zhang, H.J. (2000), "Complex turbulent wakes generated by two and three side-by-side cylinders", *International Journal of Heat and Fluid Flow*, 21, pp.125-133.